

Radiogenic Os in primitive basalts from the northwestern U.S.A.: Implications for petrogenesis

William K. Hart ^a, Richard W. Carlson ^{b,*}, Steven B. Shirey ^b

^a *Geology Department, Miami University, Oxford, OH 45056, USA*

^b *Department of Terrestrial Magnetism, Carnegie Institution of Washington, 5241 Broad Branch Road, N.W., Washington, DC 20015, USA*

Received 11 December 1996; accepted 3 April 1997

Abstract

Chemically primitive late Cenozoic tholeiitic basalts from the northwestern U.S.A. have Os-isotopic compositions more radiogenic than observed for most basalts from the ocean basins. This result is inconsistent with the simple petrogenetic model that explains the geographically correlated Sr-, Nd- and Pb-isotopic variation in these basalts as resulting solely from melting of metasomatized lithospheric mantle peridotite of varying age across this area. A magma source composed of a mixture of peridotite and pyroxenite/eclogite also fails because at the high percentage of mafic component required to explain the observed Nd–Os isotope systematics, this mixed source would not produce melts that match the major- and trace-element compositions of the observed olivine tholeiites. A more likely explanation for the observed isotopic compositions involves interaction of sublithospheric primary melts that are similar in composition to mid-ocean ridge basalt (MORB) with high-¹⁸⁷Os/¹⁸⁸Os materials in the lower crust or lithospheric mantle. Though not uniquely defined, mass-balance calculations suggest that the lithospheric component is mafic–potassic in composition, possibly a small-volume melt of mafic material in the lower crust or upper mantle. If the radiogenic Os is attributable to such interaction, the isotopic compositions of the tholeiites can be satisfied by 2–25% addition of the lithospheric component to a primitive MORB parental magma. These results show that the Os-isotope system in continental basalts can provide a clear distinction between magmas derived by melting isotopically evolved peridotitic lithosphere and those produced from a sublithospheric primary melt contaminated by mafic material in the lithosphere. © 1997 Elsevier Science B.V.

Keywords: basalts; osmium; magma contamination; lithosphere; Western U.S.

1. Introduction

Basalts erupted in continental regions often carry trace-element and Sr-, Nd- and Pb-isotopic signatures suggestive of interaction with crustal and/or enriched lithospheric mantle components. Elucidating the details of this interaction often is ambiguous

since both crust and enriched mantle can impart similar characteristics [1]. A clear answer to this question is necessary for our understanding of the genesis of continental basaltic volcanism. Because theoretical models of mantle melting suggest that dry lithospheric mantle is too cold to provide significant volumes of basaltic melt [2,3], one interpretation is that lithospheric signatures in continental basalts are primarily signs of contamination of sublithospheric melts by either lithospheric mantle or continental

* Corresponding author. Fax: +1-202-364-8726.

crust. Another interpretation is that melting of continental lithosphere is aided by the presence of water and/or low-melting temperature mafic veins that will allow the lithospheric mantle to be the main, or sole, contributor to continental basaltic volcanism in areas of extensional tectonism [4,5].

In an attempt to resolve this dilemma, we have determined the Os-isotopic composition of a set of high-Mg, “primitive”, tholeiitic basalts from the northwestern U.S.A. These basalts previously were studied for their major- and trace-element and O-, Sr-, Nd- and Pb-isotopic characteristics [6]. The limited elemental concentration variation and nearly invariant O-isotopic compositions of these basalts were used to argue against significant crustal contamina-

tion [6]. The basalts display a well-defined correlation between geographic position of eruption and Sr-, Nd- and Pb-isotopic composition that was interpreted as reflecting a change in lithospheric mantle source from young, newly accreted, lithosphere in the west to old, isotopically evolved, lithospheric mantle in the east [6].

We have returned to these basalts for Os-isotope analysis because Os should be particularly sensitive at resolving magma components derived from lithospheric peridotite as opposed to crustal material. Lithospheric peridotites tend to have unradiogenic Os independent of their Sr-, Nd- and Pb-isotopic composition [7,8], whereas crustal materials tend toward radiogenic Os. A possible caveat to this

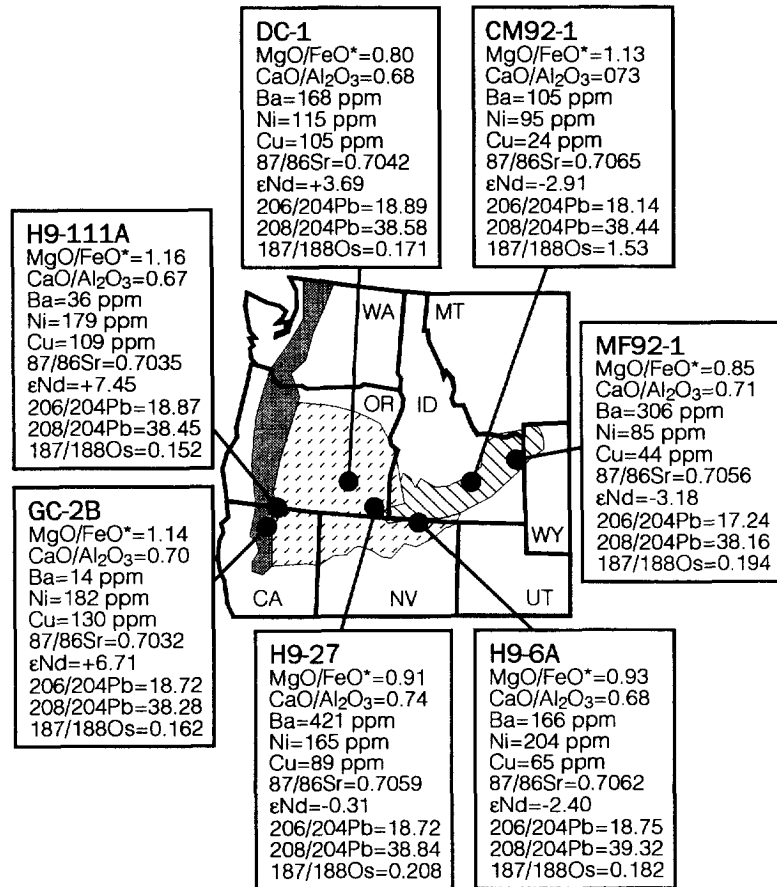


Fig. 1. Locations for the seven HAOT samples studied in this work are plotted with respect to the major physiographic and tectonic provinces of the northwestern U.S.A. including: *light shading*, Cascade volcanic arc; *stippled pattern*, Oregon Plateau; *diagonal line pattern*, Snake River Plain.

simple distinction between crust and mantle, that will be discussed in some detail, is the role played by mafic veins or layers in generally peridotitic mantle. Such mafic material will have high Re/Os and potentially radiogenic Os [9–11].

2. Review of sample characteristics

Late Cenozoic basaltic volcanism in the north-western U.S.A. has been variously ascribed to subduction-related arc, extensional back-arc, and mantle

Table 1
Elemental and Sr-, Nd-, Pb-isotope data

Sample	GC-2B	H9-111A	DC-1	H9-27	H9-6A	CM92-1	MF92-1
Longitude (°W)	121.63	121.58	118.75	117.33	115.33	113.48	111.40
Age (Ma)	0	2.69	0	5.04	5.08	0.5	0.5
SiO ₂	47.43	47.93	47.43	47.71	46.75	47.52	47.29
TiO ₂	0.69	0.68	1.25	0.81	1.19	0.99	1.59
Al ₂ O ₃	16.86	17.27	16.75	16.54	16.54	15.92	15.41
Fe ₂ O ₃	1.86	1.87	1.68	1.63	2.74	1.20	3.62
FeO	7.44	7.20	9.08	8.72	8.00	8.62	7.95
MnO	0.16	0.16	0.18	0.17	0.16	0.17	0.18
MgO	10.36	10.29	8.47	9.22	9.76	10.95	9.57
CaO	11.74	11.59	11.36	12.19	11.31	11.65	10.96
Na ₂ O	2.34	2.25	2.90	2.29	2.20	1.91	2.21
K ₂ O	0.10	0.09	0.35	0.11	0.17	0.11	0.38
P ₂ O ₅	0.07	0.06	0.14	0.11	0.21	0.08	0.26
LOI	0.51	0.59	1.02	0.89	0.79	0.80	0.79
<i>Total</i>	99.56	99.98	100.61	100.39	99.82	99.92	100.21
Rb	1.9	0.9	4.4	1.6	2.3	1.9	7.2
Sr	164	261	274	174	182	154	234
Ba	14	36	168	421	166	105	306
Zr	34	37	80	51	75	68	145
Y	20	20	25	22	24	14	27
Nb		< 1	3.8	2.2	5.4	4.1	12
Pb		0.58		0.89	1.76	0.75	0.22
Nd	4.59	4.11	7.05	6.14	11.9	3.86	18.4
Sm	1.67	1.53	2.21	1.91	3.11	1.28	4.29
Ni	182	179	115	165	204	95	85
Cr	199	277	226	298	409	511	487
V	200	224	279	235	233	234	281
Sc	39	42	41	40	32	37	37
Cu	130	109	105	89	65	24	44
MgO/FeO*	1.137	1.158	0.800	0.905	0.933	1.129	0.854
CaO/Al ₂ O ₃	0.696	0.671	0.678	0.737	0.684	0.732	0.711
K ₂ O/P ₂ O ₅	1.429	1.500	2.500	1.000	0.810	1.375	1.462
⁸⁷ Sr/ ⁸⁶ Sr	0.70320	0.70348	0.70418	0.70591	0.70616	0.70654	0.70562
¹⁴³ Nd/ ¹⁴⁴ Nd	0.512982	0.513020	0.512827	0.512622	0.512515	0.512489	0.512475
²⁰⁶ Pb/ ²⁰⁴ Pb	18.723	18.866	18.885	18.715	18.748	18.143	17.238
²⁰⁷ Pb/ ²⁰⁴ Pb	15.547	15.608	15.593	15.631	15.674	15.606	15.476
²⁰⁸ Pb/ ²⁰⁴ Pb	38.281	38.452	38.580	38.838	39.318	38.436	38.162

Major- (wt%) and trace- (ppm) element data by XRF. Rb, Sr, Sm and Nd concentrations by isotope dilution. Sr-, Nd- and Pb-isotopic compositions for all samples except MF92-1 and CM92-1 from [6].

plume related magma generation [12,13]. For the purposes of this study, we concentrate primarily on basalts from a west to east transect beginning just east of the Cascades, extending across the Oregon Plateau, and ending in the eastern Snake River Plain (Fig. 1).

Most samples studied here derive from the Oregon Plateau which is bounded by the flood basalts of the Columbia Plateau to the north, the active Cascade arc to the west, the Basin and Range proper to the south and southeast, and the Snake River Plain to the east. Since its inception as a continental extensional basin approximately 15–17 Ma ago, the Oregon Plateau has been host to widespread basalt-dominated bimodal volcanism [14]. The early history (e.g., 12 to 17 Ma) of volcanism in this area is marked by the eruption of large volumes of evolved, Fe-rich, flood basalts, such as those found at Steens Mountain. Since approximately 11 Ma ago, the most widespread magma type erupted on the Oregon Plateau is a little fractionated, mid-ocean ridge basalt (MORB)—like high-alumina olivine tholeiite, previously designated as HAOT [15]. HAOT not only is widespread throughout the Oregon Plateau [15,16], but is found to the west in the Cascades [15,17,18] to the north and northeast in the Picture Gorge and Powder River basalts [19,20], and along the Snake River Plain as far east as Yellowstone [21]. While HAOT eruptions occurred across a large area, the total volume of HAOT erupted over the last 11 Ma is small (< 1%) in comparison to the volume of basalt erupted during the ca. 15–17 Ma flood basalt episode.

An important feature of the distribution of HAOT is that it erupted in a variety of physiographic/tectonic environments; from young accreted or newly formed lithosphere of oceanic affinity in the western portion of its occurrence to ancient cratonic lithosphere to the east [14,22]. In all cases, HAOT eruptions are associated with structural features indicative of local or regional crustal extension. As a magma type, HAOT is remarkably uniform in bulk chemical composition, with primitive end-member varieties present throughout its aerial distribution (Fig. 1; Table 1). Primitive HAOT composition liquids are near saturation with olivine, orthopyroxene, augite, plagioclase and spinel at about 1.1 GPa [23], indicating either melting of a mantle source at depths as shallow as 30–35 km or crystallization of a more

primitive magma en route through the lithospheric mantle. Many HAOT display a small positive Eu anomaly [16] suggestive of interaction with plagioclase that also supports a shallow last equilibration for these magmas.

These characteristics, together with systematic regional Sr-, Nd- and Pb-isotopic variations led to a working model that calls for HAOT derivation from primarily oceanic-type mantle in the west, and primarily ancient lithospheric mantle to the east within the Snake River Plain [6]. How such petrologically similar magma can arise from such diverse sources is a challenge to explain. At least the most primitive HAOT appear to have experienced little, if any, post-generation crustal contamination, although recently this interpretation has been questioned [20], and will be further examined in this study. The wide distribution, primitive nature, and systematic Sr-, Nd- and Pb-isotopic variations make HAOT an ideal candidate for evaluating their Re–Os isotope systematics and the implications they may have for petrogenesis of continental basaltic volcanism.

3. Analytical details

Seven HAOT samples, all younger than 6 Ma, chosen to represent a west to east transect across the main region of HAOT occurrence, have been analyzed for Re and Os concentrations and Os-isotopic composition. Important bulk chemical, trace-element and isotopic characteristics for the HAOT are summarized in Fig. 1 and Table 1.

Re and Os analyses were carried out using either HF–HCl digestions in Teflon vessels [24] or aqua-regia digestions in sealed Carius tubes [25]. Os was separated after dissolution by distillation from 5 N H₂SO₄ and Re separated from the distillation residue by anion-exchange chromatography using the techniques described in [24] and [25].

Multiple dissolutions of the same sample powders show Re concentration reproducibility of $\pm 1\%$ or better, independent of dissolution technique, while Os concentration varies more widely. Samples digested in Carius tubes tend towards higher Os concentrations, but not for all samples. Given the good reproducibility of Re concentrations independent of digestion technique, we suspect that the variation in Os concentrations may relate to occasional incom-

plete spike-sample equilibration during the HF–HCl digestions [25], to inhomogeneous distribution of ultra-trace Os-rich phases in these very low-Os content rocks, or to dissolution of relatively Os-rich PGE alloys that are soluble in aqua regia, but not HF–HCl. During the course of these measurements, processing blanks were Re = 20 pg, Os = 5 pg for

the HF–HCl digestion and Re = 2 pg, Os = 2 pg for Carius tube digestions. The $^{187}\text{Os}/^{188}\text{Os}$ measured for the chemical processing blank is 0.18. Re- and Os-isotopic compositions were determined by negative ion thermal ionization mass spectrometry. Details of this procedure, as applied at DTM, are described by Shirey [26]

Table 2
HAOT Re–Os data

Sample/method	[Re](ppb)	[Os] (ppb)		$^{187}\text{Re}/^{188}\text{Os}$	$^{187}\text{Os}/^{188}\text{Os}$		
		measured	blank corr.		measured	blank corr.	initial
H9-111A							
AD1	n.d.	0.0896	0.0884	n.d.	0.1520 ± 0.0006	0.1517	0.1507
AD2	0.3965	0.0545	0.0534	35.9	0.1514 ± 0.0050	0.1508	0.1493
AD3	0.3964	0.0502	0.0498	38.7	0.1532 ± 0.0009	0.1530	0.1513
CT	0.3991	0.2099	0.2084	9.25	0.1551 ± 0.0003	0.1550	0.1546
GC-2B							
AD1	n.d.	0.0122	0.0113	n.d.	0.1634 ± 0.0041	0.1619	0.1619
AD2	0.2658	0.0108	0.0101	127	0.1627 ± 0.0039	0.1615	0.1615
DC-1							
AD1	n.d.	0.0575	0.0566	n.d.	0.1700 ± 0.0019	0.1698	0.1698
AD2	0.5768	0.0212	0.0204	137	0.1713 ± 0.0008	0.1710	0.1710
CT	0.5752	0.0837	0.0830	33.6	0.1708 ± 0.0009	0.1708	0.1708
H9-27							
AD1	0.4860	0.0460	0.0452	52.4	0.2086 ± 0.0010	0.2092	0.2049
AD2	0.4896	0.0454	0.0450	53.1	0.2066 ± 0.0018	0.2070	0.2026
CT	0.4870	0.0676	0.0673	35.3	0.2186 ± 0.0005	0.2190	0.2161
H9-6A							
AD1	0.3109	0.0930	0.0921	16.4	0.1780 ± 0.0008	0.1780	0.1766
AD2	0.3066	0.0474	0.0462	32.1	0.1863 ± 0.0103	0.1865	0.1838
CT	0.3040	0.0922	0.0916	16.1	0.1876 ± 0.0038	0.1876	0.1863
CM92-1							
AD1	0.1390	0.0017	0.0014	566	1.1875 ± 0.0110	1.606	1.602
AD2	n.d.	0.0013	0.0010	n.d.	0.9933 ± 0.0060	1.472	1.465
CT1	n.d.	0.0057	0.0039	n.d.	1.2331 ± 0.1740	1.914	1.909
MF92-1							
AD1	0.1151	0.0040	0.0030	186	0.1950 ± 0.0184	0.1998	0.1983
AD2	n.d.	0.0037	0.0034	n.d.	0.1898 ± 0.0009	0.1913	0.1898

AD corresponds to HF–HCl digestion, CT to Carius tube digestion.

4. Results

As shown in Table 2, the basalts display a wide range in Os concentration (0.0010–0.208 ppb), but a restricted range in Re content (0.12–0.58 ppb) averaging 0.33 ± 0.17 (1σ) ppb. The average Re content of HAOT is similar to that of average ocean island basalt (Re = 0.26 ± 0.12 ppb, when corrected for olivine fractionation to a Mg# of 0.73 [27]), but lower than the MORB average Re content of 0.93 ± 0.34 ppb [27]. Re concentrations show vague correlations (e.g., correlation coefficient > 0.7) only with the elements Al, Na and Cr and the poorest correlations with the highly incompatible elements K and Ba. There is no correlation of Os concentration with the concentration of other elements (e.g., Cu, Ni, Fe) that might be sensitive to possible fractionation of sulfide phases from these magmas.

Re and Os concentration variations also are independent of geographic location, as is the case for most other HAOT elemental parameters. Three exceptions are noted. Al_2O_3 and Cu display systematic decreases from west to east while Cr increases to the east (Fig. 2). At present, these trends are difficult to interpret given the otherwise homogeneous nature of HAOT across the entire region, but they may suggest an eastward increasing role of pyroxene over plagioclase during HAOT evolution. This, in turn, may be indicative of increasing depths of melting and/or fractionation.

HAOT Re and Os concentrations are within the range reported for oceanic basalts, whereas their Os-isotopic compositions are more radiogenic. Only one sample (H9-111A) has $^{187}\text{Os}/^{188}\text{Os}$ within the range observed for ocean island basalts [28–33]. Ocean island basalts with Os as radiogenic as found for H9-111A, however, either yield Pb-isotopic signatures very different from H9-111A (e.g., HIMU island of Mangaia [33]) or are considered to have been affected by interaction with old, radiogenic oceanic crust beneath the volcano [30,31,34]. Some MORB have $^{187}\text{Os}/^{188}\text{Os}$ high enough to overlap the HAOT values reported here [35]. Since MORB have extremely low Os concentrations [36], there is considerable uncertainty as to whether the more radiogenic values (e.g., $^{187}\text{Os}/^{188}\text{Os}$ 0.135) reported for MORB represent igneous values, seawater alteration [35], or in-situ Re decay. Abyssal peridotites,

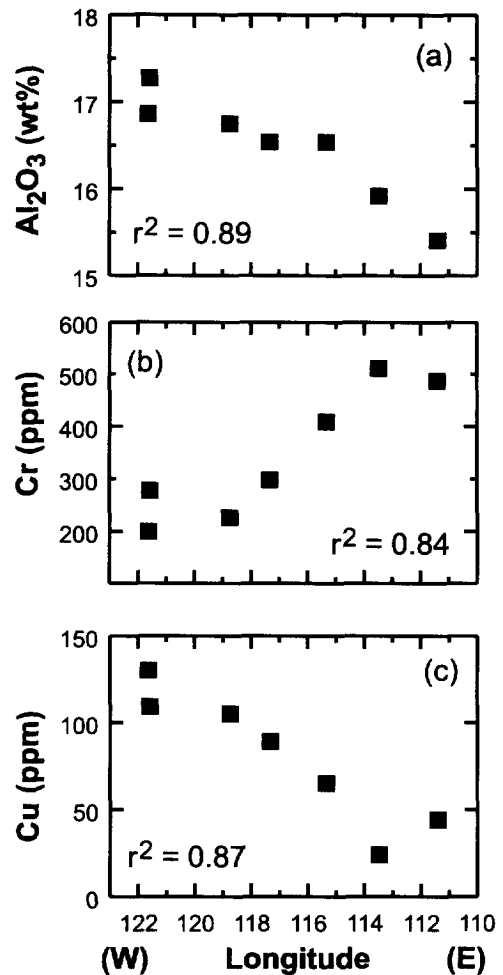


Fig. 2. Compositional characteristics of the studied HAOT that correlate with geographic position of eruption of the individual samples.

which have Os contents high enough to be relatively insensitive to seawater Os addition, have $^{187}\text{Os}/^{188}\text{Os} < 0.127$, well below the HAOT compositions [29,35,37]. In addition, peridotite xenoliths from the Simcoe volcano in the Cascades have $^{187}\text{Os}/^{188}\text{Os} < 0.131$ [38], again well below even the least radiogenic Os seen for the HAOT.

No consistent relation between Os concentration, Re/Os or $^{187}\text{Os}/^{188}\text{Os}$ are observed in the HAOT, although the lowest-Os content HAOT yields the highest $^{187}\text{Os}/^{188}\text{Os}$ (CM92-1) and the highest-Os content sample yields the lowest $^{187}\text{Os}/^{188}\text{Os}$ (H9-111A). $^{187}\text{Os}/^{188}\text{Os}$ increases from west to east

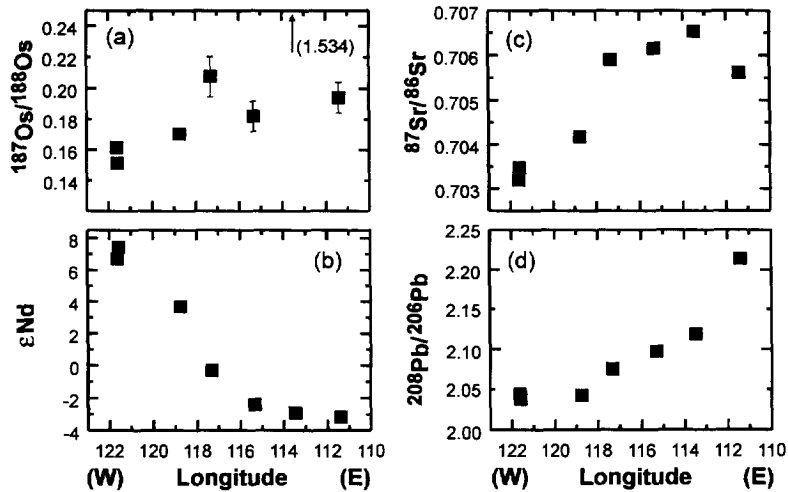


Fig. 3. Isotopic variation of the HAOT from west to east across the sample area.

across the sample area (Fig. 3), but the trend is punctuated by two samples offset to much more radiogenic Os. The eastward increase in $^{187}\text{Os}/^{188}\text{Os}$ is akin to previously observed longitudinally correlated changes in Sr-, Nd- and Pb-isotopic compositions (Fig. 3) documented for a larger suite of HAOT, as well as for other late-Cenozoic volcanic products in this region.

5. Discussion

HAOT share many chemical similarities with MORB or primitive island arc tholeiites, but have regionally varying Sr-, Nd- and Pb-isotopic compositions that distinguish them from any oceanic basalt. The radiogenic Os found for the HAOT analyzed here further enhance this distinction (Fig. 4). Estimates of the Os-isotopic composition of undifferentiated mantle range from $^{187}\text{Os}/^{188}\text{Os} = 0.1287$ to as high as 0.132 based, respectively, on chondritic analogs for mantle Re and Os abundances [39] and on the Os-isotopic composition range observed for ocean island basalts [29]. Thus, the HAOT data require identification of a source of radiogenic Os that is either in the source of the parental magmas or is added by contamination at some stage during the transit from source to eruption.

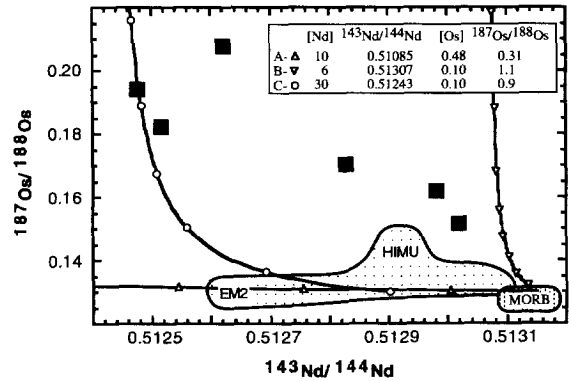


Fig. 4. Os–Nd isotope mixing systematics for the addition of different radiogenic Os components to peridotite. For curves A and B, the peridotite has [Nd]=1.5 ppm, $^{143}\text{Nd}/^{144}\text{Nd} = 0.51315$, [Os]=3 ppb, $^{187}\text{Os}/^{188}\text{Os} = 0.13$. The Nd and Os concentrations and isotopic compositions listed in the figure for component A are those of a websterite xenolith from the Highwoods Mountains of Montana [10]; for component B, a websterite xenolith from Chino Valley Arizona [46]; and component C is a hypothetical composition chosen to approximate a subduction-related mixture of altered oceanic crust and pelagic sediment. The peridotite end-member for component C has Os concentration reduced to 0.65 ppb, Nd increased to 2 ppm with $^{143}\text{Nd}/^{144}\text{Nd} = 0.5129$ to approximate the average composition of arc-mantle peridotite xenoliths from Simcoe volcano in the Cascades [38]. Large squares show the data for HAOT excluding sample CM92-1 which plots at $^{187}\text{Os}/^{188}\text{Os} = 1.5$ with $^{143}\text{Nd}/^{144}\text{Nd} = 0.51249$. Symbols along the curves denote 2% additions of contaminant for curve A, and 10% additions for curves B and C. Nd concentrations listed in the figure are in ppm while those for Os are in ppb.

Because of the moderately incompatible nature of Re, but compatible behavior of Os during melting of mantle peridotite, melt extraction from the mantle generally leaves behind Re-depleted peridotites that will evolve less radiogenic Os than undifferentiated mantle. If the higher $^{187}\text{Os}/^{188}\text{Os}$ measured for some MORB are ascribed to seawater contamination [35], Re removal accompanying past melt depletion probably explains the lower than “bulk-mantle” Os-isotopic compositions observed for MORB-related oceanic peridotites. In addition, Re-depleted peridotites, some with very low $^{187}\text{Os}/^{188}\text{Os}$, are a pervasive component of cratonic lithospheric mantle and seem to retain their unradiogenic Os even if affected by later metasomatic events that raise their incompatible-element contents and lead to evolved Sr-, Nd- and Pb-isotopic compositions [7,8,10].

An exception to this simple model of Re depletion by melt extraction might occur in convergent margin settings where more oxidizing melting conditions in the mantle wedge above the subducting plate may promote decomposition of Os-bearing phases in the peridotite with resultant loss of Os [38]. Relatively low Os concentrations (0.3–1.0 ppb) have been reported for peridotite xenoliths from the Simcoe volcano in the Washington Cascades, but these samples also have Re/Os near or below bulk-Earth values and $^{187}\text{Os}/^{188}\text{Os} < 0.131$ [38]. Consequently, radiogenic Os is not expected, nor has it been observed, in mantle peridotite. Thus, the radiogenic Os-isotopic compositions found for HAOT deny simple petrogenetic models that describe HAOT as unfractionated, uncontaminated, melts of peridotitic mantle.

5.1. A mafic, not peridotitic, source for HAOT?

An interesting possibility to consider is that the source of HAOT is predominantly mafic composition material in the upper mantle or lower crust. In many respects, the composition of HAOT, particularly the low Ti and high Al contents, mirror the composition of primitive island arc tholeiites that some have argued derive from melting a quartz-eclogite, rather than peridotitic, source [40]. While not directly related to subduction zone volcanism, HAOT occur in an area with an extensive magmatic history ranging from Mesozoic to Recent arc-, Miocene

flood basalt-, and Miocene to Recent extensional-volcanism. The long magmatic history of this area could provide sufficient mafic material in the lower crust–upper mantle to serve as potential source material for HAOT during late Cenozoic extension [5]. Indeed, some workers have suggested that the largest volume of basalt in this area, the Columbia River flood basalts, derive from the melting of a pyroxene-rich, mafic source [41,42].

A relatively young mafic component is required by the HAOT data to explain the quite high $^{143}\text{Nd}/^{144}\text{Nd}$ yet high $^{187}\text{Os}/^{188}\text{Os}$ found for the sample with least radiogenic Os, H9-111A. For example, a mafic material could evolve $^{187}\text{Os}/^{188}\text{Os}$ from 0.13 to the 0.151 found for H9-111A in only 15 Ma given a high, but not unreasonable, $^{187}\text{Re}/^{188}\text{Os}$ of 84 and would require a $^{187}\text{Re}/^{188}\text{Os}$ of only 13 to create this Os-isotopic difference in 100 Ma. For time periods of 100 Ma or less, given the likely Rb/Sr, Sm/Nd and U/Pb of potential source materials for HAOT, only imperceptibly small changes would occur in Sr-, Nd- and Pb-isotopic composition. Older mafic components would likely evolve sufficiently distinct Sr-, Nd- and Pb-isotopic compositions as to cause greater offsets from “oceanic” values than observed in the least isotopically evolved HAOT.

Several characteristics of the HAOT compositions, however, are hard to reconcile with a purely mafic source. First is the issue of whether a mafic source could produce melts with the “primitive” compositional features of HAOT, e.g. high Mg/Fe, high Ni and Cr? In other words, can one produce a primitive high-alumina olivine tholeiite composition by melting a basaltic source? Though we consider mafic source materials an often overlooked, but potentially important, component for other types of continental volcanism [43], HAOT major-element compositions have yet to be produced by melting mafic sources [44]. Second, the very low contents of highly incompatible elements (e.g., Rb, Ba) observed for the most primitive HAOT are unlikely to result from melting a mafic, as opposed to ultramafic, source. Finally, the observed correlation between Os- and Nd-isotopic variation would require a surprisingly regular change in Re/Os or age across the area of HAOT occurrence.

5.2. Nd–Os isotope mixing systematics

The Os data for HAOT show a general eastward increase in $^{187}\text{Os}/^{188}\text{Os}$ that follows the previous geographically correlated trends observed in the Sr-, Nd- and Pb-isotopic composition of these basalts (Fig. 3). To address the cause of this variation, we explore HAOT isotope systematics in terms of interaction between various source and contaminant compositions that are likely to be present in the mantle and crust across this area as outlined by previous Sr-, Nd- and Pb-isotopic studies of basalts from the Pacific Northwest [45]. Because the range of Sm/Nd in rocks is much more limited, and more predictable, than Rb/Sr and U/Pb variation, we will focus our discussion on the implication of the observed Nd- and Os-isotopic variation in HAOT for the petrogenesis of these lavas.

Compared to most melt compositions, mantle peridotite will have low Nd, but high Os concentrations. Consequently, mixing trajectories on plots of Nd- vs. Os-isotopic composition will be quite different in cases where the radiogenic Os component is introduced as a source component (e.g., mafic veins in a peridotitic mantle source) as opposed to contamination of a melt, for example, in a crustal magma chamber. This is shown in Figs. 4 and 5 by consideration of a number of hypothetical mixing models. All models start with a peridotitic source or parental melt with Nd- and Os-isotopic compositions similar to those expected for northern Pacific MORB. A peridotitic source with “plume” isotopic characteristics similar to FOZO [33] could be substituted with little effect on the following arguments. Since there is little or no direct information on the characteristics of the source of radiogenic Os in these samples, the following models consider first the rough systematics of mixing in the Os–Nd isotope systems to illustrate the requirements imposed by the data on the nature of the mixing components.

5.2.1. Source contamination

In the source contamination models, peridotite is mixed with hypothetical “mafic vein” materials. Fig. 4 shows the isotopic effects caused by mixing peridotite with: (A) a websterite xenolith from the shallow mantle beneath Montana [10]; (B) a websterite xenolith from the mantle beneath central Ari-

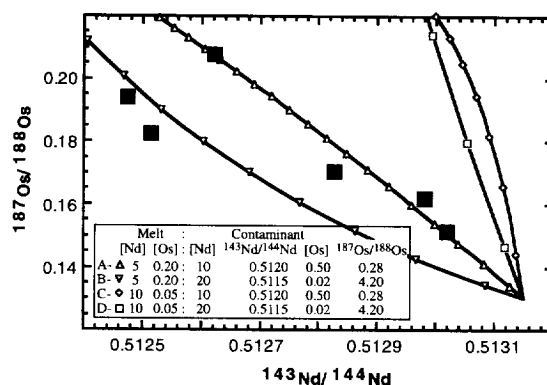


Fig. 5. Os–Nd isotope mixing curves expected for contamination of both primitive and evolved basaltic melts by various hypothetical components likely to reside in the lithosphere of this region. The *large squares* show the data for the analyzed HAOT with the exception of sample CM92-1. *Symbols* along the curves denote 2% increments in the amount of contaminant in the mixture. Nd concentrations listed in the figure are in ppm while those for Os are in ppb.

zona [46]; and (C) a hypothetical composition selected to represent a possible subduction component derived from pelagic sediment. While none of these “contaminant” compositions necessarily must be present in the area of the HAOT sources, they represent a fair range of compositions for underplated mafic melts and/or subduction-derived fluids that might be present given the geologic history of this region. They also cover a wide range in Nd and Os concentrations and isotopic compositions to illustrate the effects of such variations on the mixing curves.

For this type of source contamination, because of the very low Nd/Os of the peridotite compared to all “contaminants”, the mixing trajectories in Os–Nd isotope space (Fig. 4) are strongly hyperbolic with rapid deflection in Nd-isotopic composition, but little change in Os-isotopic composition until the Nd-isotopic composition of the contaminant is approached. As seen in Fig. 4, 6% addition of the Montana websterite xenolith to peridotite will cause the Nd-isotopic composition of the mixture to equal that of the lowest $^{143}\text{Nd}/^{144}\text{Nd}$ measured for samples in this study, yet the $^{187}\text{Os}/^{188}\text{Os}$ will change only from 0.130 to 0.132. More dramatic shifts in Os-, compared to Nd-, isotopic composition can be achieved if the mafic component is assumed to be less LREE enriched, such as for the example using

the Arizona websterite, but no single mafic component can recreate the shallow slope of the Nd–Os correlation displayed by the HAOT data. This is particularly true in the example using the “subduction component”, even if the Os concentration of the peridotite is lowered to the 0.65 ppb average obtained by Brandon et al. [38] for Simcoe peridotite xenoliths. Consequently, the mixing relationships shown in Fig. 4 provide a strong argument that the eastward increase in $^{187}\text{Os}/^{188}\text{Os}$ observed in the HAOT is not caused by melting a source consisting of varying amounts and/or age of high- $^{187}\text{Os}/^{188}\text{Os}$ mafic veins in a generally low- $^{187}\text{Os}/^{188}\text{Os}$ peridotitic matrix.

5.2.2. Melt contamination

The shallow-sloped correlation between Nd- and Os-isotopic composition displayed by the HAOT data, with the notable exception of sample CM92-1 which has extremely radiogenic Os, suggests that if two-component mixing is responsible for this variation, the two mixing components have similar Nd/Os concentration ratios. As indicated in the preceding discussion, this is unlikely to occur if peridotite is involved because of its low Nd/Os, but is a likely situation for interaction between a basaltic melt and most mafic to silicic igneous rock compositions that would be found in the continental lithosphere. This type of mixing, termed melt contamination, is evaluated with the models depicted in Fig. 5.

In Fig. 5, the effect of variable Nd and Os concentration in both primary melt and contaminant is shown. One set of calculations is for a relatively unevolved primary melt with low Nd concentration (5 ppm) and moderately high Os content (0.2 ppb) mixing with either hypothetical “primitive” ([Nd] = 10 ppm, [Os] = 0.5 ppb) or “evolved” ([Nd] = 20 ppm, [Os] = 0.2 ppb) contaminants. The second set of curves considers contamination of a more evolved melt with [Nd] = 10 ppm and [Os] = 0.05 ppb. The Os-isotopic composition of the contaminants is calculated assuming a constant Re concentration of 0.5 ppb and an age of 2 Ga. Varying the age of the contaminant primarily will change the percentage of contaminant required to reach any point on the mixing curves shown in Fig. 5, but will not greatly modify their shape. Thus, the varying age of the crustal basement across the area of HAOT occur-

rence is unlikely to significantly modify conclusions about the nature of mixing end-members that are derived from the shape of the mixing curves in comparison to the HAOT data.

These models of melt contamination produce relatively linear mixing curves in Fig. 5, but with considerably different slopes depending on whether the melt undergoing contamination is “primitive”, with high Os and low Nd contents, or “evolved”, with high Nd and low Os. The two curves calculated assuming simple binary mixing of a primitive magma with either contaminant pass through the data for most of the HAOT. For the compositions modeled in Fig. 5, the sample with highest $^{143}\text{Nd}/^{144}\text{Nd}$ requires 3–7% contamination to explain its Nd- and Os-isotopic compositions starting from a MORB parent magma, whereas 16–40% contaminant is required to reach the isotopic composition of the sample with lowest $^{143}\text{Nd}/^{144}\text{Nd}$. Clearly, these mixing percentages depend strongly on the Nd and Os concentration and isotopic composition of the end-members, but demonstrate that the Nd–Os correlation found for the HAOT, with the exception of CM92-1, can be reproduced by contamination of primitive MORB-like magmas. The Os–Nd correlation shown in Fig. 5 is too crude to allow distinction between a MORB or OIB primary magma on the basis of isotopic composition. However, the shallow slope of the data in Fig. 5 is most easily explained if the primary magma has Nd concentration of 5 ppm or less, as observed for some HAOT (Table 1), which is more similar to typical primitive-MORB compositions than to most OIB.

The very radiogenic Os found for sample CM92-1 is unlikely to reflect greater degrees of contamination than for other HAOT because CM92-1 has among the lowest LIL-element contents of the HAOT studied here. In the mixing models shown in Fig. 5, to reach the extreme Os-isotopic composition observed for CM92-1 could be accomplished by: lowering the Os concentration of the starting magma; raising the Os concentration of the contaminant; or raising the $^{187}\text{Os}/^{188}\text{Os}$ of the contaminant. If the magma undergoing mixing started with 0.01 ppb Os or 0.001 ppb Os, instead of the 0.05 ppb Os used in case D in Fig. 5, to produce the Os-isotopic composition of CM92-1 would require 20% or 2% contaminant, respectively, in the mixture. Alternatively, if

the $^{187}\text{Os}/^{188}\text{Os}$ of the contaminant were increased from 4.2 to 10, the amount of contaminant needed to explain the Os-isotopic composition of CM92-1 in the mixing model of Fig. 5, case D, would decrease from 55% to 30%. These calculations demonstrate the sensitivity of the Os-isotope system in reflecting contamination of low-Os content melts.

5.3. Implications for HAOT petrogenesis

Fig. 6 and Table 3 present the results of a numeric mixing model using mixing components chosen to reflect the varying age of the lithosphere throughout the area of HAOT occurrence as well as the isotopic end-members identified by previous Sr-, Nd- and Pb-isotopic studies of the basalts of the Pacific Northwest [6,14,45]. A three-component mixing model was employed to account for contamination of low- $^{187}\text{Os}/^{188}\text{Os}$ MORB melts (the C1 component of [45]) by material with more radiogenic Os derived

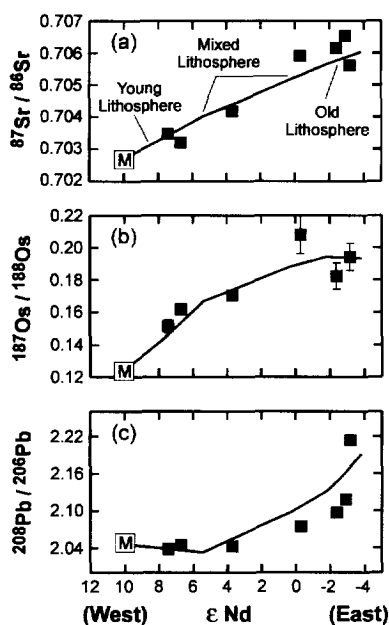


Fig. 6. Results of a three-component mixing model using the end-member compositions given in Table 3. This model approximates the changing age and composition of the lithosphere across the area of HAOT occurrence based on Sr-, Nd- and Pb-isotope variation observed in many basalts from the Pacific Northwest [14,45]. $^{208}\text{Pb}/^{206}\text{Pb}$ is plotted because it simultaneously illustrates the geographically correlated changes in $^{206}\text{Pb}/^{204}\text{Pb}$ and $^{208}\text{Pb}/^{204}\text{Pb}$ that occur in basalts of this region.

Table 3

Ternary mixing model

	MORB melt (C1)	Mafic Young (west) (C2)	Contaminant Old (east) (C3)
End-member parameters			
[Sr] (ppm)	120	320	230
$^{87}\text{Sr}/^{86}\text{Sr}$	0.70270	0.70600	0.71300
[Nd] (ppm)	5	15	15
$^{143}\text{Nd}/^{144}\text{Nd}$	0.51315	0.51260	0.51150
[Pb] (ppm)	0.5	4	4
$^{206}\text{Pb}/^{204}\text{Pb}$	18.8	19.1	16.5
$^{207}\text{Pb}/^{204}\text{Pb}$	15.5	15.5	15.5
$^{208}\text{Pb}/^{204}\text{Pb}$	38.5	38.7	37.5
[Os] (ppb)	0.05	0.10	0.10
$^{187}\text{Os}/^{188}\text{Os}$	0.125	0.250	0.330
Mixing proportions			
West—start	100	0	0
West—end	80	20	0
Middle 1—start	80	20	0
Middle 1—end	75	15	10
Middle 2—start	75	15	10
Middle 2—end	75	10	15
East—start	75	10	15
East—end	80	0	20

C1, C2, C3 correspond to the isotopic end-members defined for the Columbia River basalts [43].

from young arc-related lithosphere (C2 of [45]) and ancient (ca. 2500 Ma) cratonic lithosphere (C3 of [45]). The radiogenic Os end-member could include mafic components in the lithospheric mantle, or melts derived from them, as long as the surrounding peridotite is not significantly involved. To explain the rapid increase in $^{187}\text{Os}/^{188}\text{Os}$ from abyssal peridotite values (0.125) to the values observed in the western HAOT requires that C2 have isotopic compositions more evolved than expected for young, i.e. Cenozoic, lithosphere unless the arc basement in this area contained substantial input from fluids derived from subducted pelagic sediments [38]. The model was applied in a step-wise fashion to simulate the transition from Cenozoic to Archean lithosphere across the area of HAOT occurrence. Given the lack of direct samples of the lithospheric contaminant involved, the model is necessarily ad-hoc, but it serves to illustrate that a contamination scenario such as outlined above can be reconciled with the Sr-,

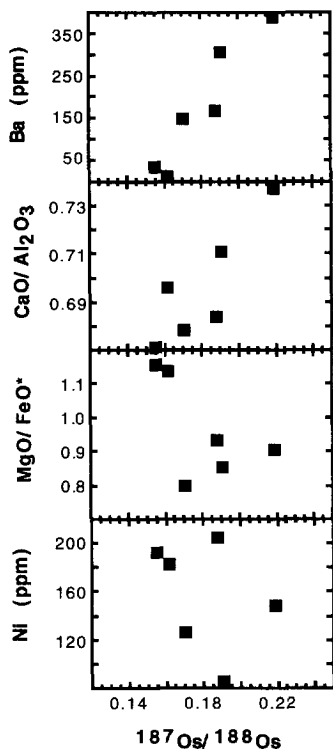


Fig. 7. Ba, CaO/Al₂O₃, MgO/FeO* and Ni concentrations of HAOT, excepting sample CM92-1, plotted against Os-isotopic composition. FeO* is total iron concentration expressed as FeO.

Nd-, Os- and Pb-isotopic variation observed in HAOT.

The isotopic results do not uniquely define the composition of the lithospheric component, but this can be investigated further by examination of the combined isotope–trace element systematics of HAOT. Of the elemental characteristics that distinguish HAOT from MORB, the most prominent is the tendency of HAOT towards relatively high Ba contents. With the exception of the extremely radiogenic sample CM92-1, the remaining samples display a good correlation between Ba content and Os-isotopic composition (correlation coefficient = 0.94, Fig. 7), suggesting that the component contributing radiogenic Os also has moderately high Ba concentration.

From the isotope mixing systematics discussed previously, the range in isotopic compositions observed for HAOT require a minimum of 15% input of the contaminant to explain the isotopic difference between the samples with highest (H9-111A) and

lowest (MF92-1) ¹⁴³Nd/¹⁴⁴Nd. To assess the allowable composition of the contaminant, we can calculate the required concentrations in the contaminant which when added to H9-111A in a 15:85 (contaminant: H9-111A) mixture produces MF92-1. For incompatible elements, the contaminant is calculated to contain 2.02 wt% K₂O, 1.4% P₂O₅, 43 ppm Rb and 1840 ppm Ba, and for TiO₂, CaO and Al₂O₃, 6.7%, 7.4% and 4.9%, respectively. The calculated contaminant composition is more similar to that of a mafic–potassic melt than to any intermediate to felsic crustal material.

A particularly sensitive indicator of contamination by intermediate to felsic crust is the K₂O/P₂O₅ ratio [14] since most evolved crustal rocks have high K₂O/P₂O₅, generally, greater than 5. Contamination of H9-111A with 15% of even a relatively primitive Cascade basaltic andesite composition would raise the K₂O/P₂O₅ of the mixture to above 3, yet only one of the HAOT analyzed here have K₂O/P₂O₅ above 1.5 (Table 1). Furthermore, HAOT show little or no correlation between isotopic composition and K₂O/P₂O₅. If any trend exists, increasing ⁸⁷Sr/⁸⁶Sr, ¹⁸⁷Os/¹⁸⁸Os, and decreasing ¹⁴³Nd/¹⁴⁴Nd tend to be accompanied by lower K₂O/P₂O₅ in HAOT.

An additional argument against the involvement of contaminants more evolved than basalt in HAOT petrogenesis is provided by the extremely rough positive correlation between Ca/Al and Os-isotopic composition in the HAOT (Fig. 7). This correlation suggests that the contaminant is not a low-Ca/Al material, chemically like pelagic sediment [20] or an evolved, e.g. intermediate to felsic, igneous composition. Obviously, the CaO and Al₂O₃ abundances of these magmas are extremely sensitive to plagioclase and pyroxene fractionation. In the HAOT, however, there is no correlation between Ca, Mg or Ni concentration with Os-isotopic composition (Fig. 7), which suggests that the contamination is not accompanied by significant removal of either olivine or pyroxene. In other words, contamination does not appear to be accompanied by fractional crystallization in HAOT genesis. This observation may support the model of HAOT genesis that involves mixing between sub-lithospheric primary magmas and low-volume melts of mafic material in the lithosphere rather than ingestion of a crustal contaminant in a cooling, fractionating, crustal magma chamber.

Based on these observations, we suggest that HAOT form as the end-product of MORB-like primary melts that suffered minor, e.g. a few percent, contamination by small-volume melts of mafic material in the lithosphere. The regional variation in isotopic composition of HAOT is then due, in this model, to progressively greater involvement of older mafic material moving from west to east. Our preference for a MORB-like, as opposed to OIB-like, primary magma is based less on the isotopic composition of HAOT than on their major- and trace-element characteristics. Primitive HAOT have Al, Ti, and Fe contents, very low alkali contents ($K_2O < 0.1\%$, $Rb < 1$ ppm) and chondrite-normalized La/Sm ratios less than one, all of which are more like MORB than ocean island tholeiites. Though we cannot unequivocally rule out the possibility that the variable isotopic compositions of HAOT result from crustal contamination, the lack of evidence for accompanying crystal fractionation, the high calculated Ca/Al and low K_2O/P_2O_5 of the contaminant, the high compatible-element contents of HAOT, and their near saturation with peridotitic mineralogy at depths of 30–35 km [23] suggest that this interaction occurred in the shallow lithospheric mantle.

Acknowledgements

This work was supported by grants from the Ohio Board of Regents and Miami University Committee on Faculty Research (W.K.H.), and grants EAR-8904596 and EAR-9204780 (W.K.H.), and EAR-9005412, EAR-9204718 and EAR-9506713 (R.W.C. and S.B.S.) from the National Science Foundation. Reviews by N. Arndt and J. Chesley detected the ambiguities in our approach to this problem which, hopefully, have now been satisfactorily resolved, or at least clearly stated. *CL*

References

- [1] R.W. Carlson, Physical and chemical evidence on the cause and source characteristics of flood basalt volcanism, *Aust. J. Earth Sci.* 38 (1991) 525–544.
- [2] N.T. Arndt, U. Christensen, The role of lithospheric mantle in continental flood volcanism: Thermal and geochemical constraints, *J. Geophys. Res.* 97 (1992) 10967–10981.
- [3] D. McKenzie, M.J. Bickle, The volume and composition of melt generated by extension in the lithosphere, *J. Petrol.* 29 (1988) 625–679.
- [4] K. Gallagher, C.J. Hawkesworth, Dehydration melting and the generation of continental flood basalts, *Nature (London)* 358 (1992) 57–59.
- [5] D.L. Harry, W.P. Leeman, Partial melting of melt metasomatized subcontinental mantle and the magma source potential of the lower lithosphere, *J. Geophys. Res.* 100 (1995) 10255–10269.
- [6] W.K. Hart, Chemical and isotopic evidence for mixing between depleted and enriched mantle, northwestern USA, *Geochim. Cosmochim. Acta* 49 (1985) 131–144.
- [7] R.J. Walker, R.W. Carlson, S.B. Shirey, F.R. Boyd, Os, Sr, Nd, and Pb isotope systematics of southern African peridotite xenoliths: Implications for the chemical evolution of subcontinental mantle, *Geochim. Cosmochim. Acta* 53 (1989) 1583–1595.
- [8] D.G. Pearson, R.W. Carlson, S.B. Shirey, F.R. Boyd, P.H. Nixon, Stabilization of Archean lithospheric mantle: a Re–Os isotope study of peridotite xenoliths from the Kaapvaal craton, *Earth Planet. Sci. Lett.* 134 (1995) 341–357.
- [9] L.C. Reisberg, C.J. Allègre, J.-M. Luck, The Re–Os systematics of the Ronda ultramafic complex in southern Spain, *Earth Planet. Sci. Lett.* 105 (1991) 196–213.
- [10] R.W. Carlson, A.J. Irving, Depletion and enrichment history of subcontinental lithospheric mantle: an Os, Sr, Nd and Pb isotopic study of ultramafic xenoliths from the northwestern Wyoming Craton, *Earth Planet. Sci. Lett.* 126 (1994) 457–472.
- [11] D.G. Pearson, G.A. Snyder, S.B. Shirey, L.A. Taylor, R.W. Carlson, N.V. Sobolev, Archean Re–Os age for Siberian eclogites and constraints on Archean tectonics, *Nature (London)* 374 (1995) 711–713.
- [12] R.L. Christiansen, E.H. McKee, Late Cenozoic volcanic and tectonic evolution of the Great Basin and Columbia Intermontane regions, *Geol. Soc. Am. Mem.* 152 (1978) 283–311.
- [13] D. Geist, M. Richards, Origin of the Columbia Plateau and Snake River Plain: deflection of the Yellowstone plume, *Geology* 21 (1993) 789–792.
- [14] R.W. Carlson, W.K. Hart, Crustal genesis on the Oregon Plateau, *J. Geophys. Res.* 92 (1987) 6191–6206.
- [15] W.K. Hart, J.L. Aronson, S.A. Mertzman, Areal distribution and age of low-K, high-alumina olivine tholeiite magmatism in the northwestern Great Basin, *Geol. Soc. Am. Bull.* 95 (1984) 186–195.
- [16] E.H. McKee, W.A. Duffield, R.J. Stern, Late Miocene and early Pliocene basaltic rocks and their implications for crustal structure, northeastern California and south-central Oregon, *Geol. Soc. Am. Bull.* 94 (1983) 292–304.
- [17] W.P. Leeman, D.R. Smith, W. Hildreth, Z. Palacz, N. Rogers, Compositional diversity of late Cenozoic basalts in a transect across the southern Washington Cascades: implications for subduction zone magmatism, *J. Geophys. Res.* 95 (1990) 19561–19582.
- [18] J.M. Donnelly-Nolan, D.E. Champion, T.L. Grove, M.B. Baker, J.E. Taggart Jr., P.E. Bruggman, The Giant Crater

- lava field: geology and geochemistry of a compositionally zoned high-alumina basalt to basaltic andesite eruption at Medicine Lake volcano California, *J. Geophys. Res.* 21 (1991) 21843–21863.
- [19] A.D. Brandon, Constraints on magma genesis behind the Neogene Cascade arc: Evidence from major and trace element variation of high-alumina and tholeiitic volcanics of the Bear Creek area, *J. Geophys. Res.* 94 (1989) 7775–7798.
- [20] D.G. Bailey, R.M. Conrey, Common parent magma for Miocene to Holocene mafic volcanism in the northwestern United States, *Geology* 20 (1992) 1131–1134.
- [21] W. Hildreth, A.N. Halliday, R.L. Christiansen, Isotopic and chemical evidence concerning the genesis and contamination of basaltic and rhyolitic magma beneath the Yellowstone Plateau volcanic field, *J. Petrol.* 32 (1991) 63–138.
- [22] W.P. Leeman, J.S. Oldow, W.K. Hart, U.S. Lithosphere-scale thrusting in the western Cordillera as constrained by Sr and Nd isotopic transitions in Neogene volcanic rocks, *Geology* 20 (1992) 63–66.
- [23] K.S. Bartels, R.J. Kinzler, T.L. Grove, High pressure phase relations of primitive high-alumina basalts from Medicine Lake volcano, northern California, *Contrib. Mineral. Petrol.* 108 (1991) 253–270.
- [24] R.J. Walker, Low-blank chemical separation of rhenium and osmium from gram quantities of silicate rock for measurements by resonance ionization mass spectrometry, *Anal. Chem.* 58 (1988) 2923–2927.
- [25] S.B. Shirey, R.J. Walker, Carius tube digestions for low-blank rhenium–osmium analysis, *Anal. Chem.* 67 (1995) 2136–2141.
- [26] S.B. Shirey, Re–Os isotopic compositions of midcontinent rift system picrites: implications for plume–lithosphere interaction and enriched mantle sources, *Can. J. Earth Sci.* (1997) in press.
- [27] E.H. Hauri, S.R. Hart, Rhenium abundances and systematics in oceanic basalts, *Chem. Geol.* 139 (1997) 185–204.
- [28] M. Roy-Barman, C.J. Allègre, $^{187}\text{Os}/^{186}\text{Os}$ in oceanic island basalts: tracing oceanic crust recycling in the mantle, *Earth Planet. Sci. Lett.* 129 (1995) 145–161.
- [29] C.E. Martin, Os isotopic characteristics of mantle derived rocks, *Geochim. Cosmochim. Acta* 55 (1991) 1421–1434.
- [30] L. Reisberg, A. Zindler, F. Marcantonio, W. White, D. Wyman, B. Weaver, Os isotope systematics in ocean island basalts, *Earth Planet. Sci. Lett.* 120 (1993) 149–167.
- [31] E. Widom, S.B. Shirey, Os isotope systematics in the Azores: implications for mantle plume sources, *Earth Planet. Sci. Lett.* 142 (1996) 451–465.
- [32] F.A. Marcantonio, A. Zindler, H. Staudigel, H. Schmincke, Os isotope systematics of La Palma, Canary Islands: evidence for recycled crust in the mantle source of HIMU ocean islands, *Earth Planet. Sci. Lett.* 133 (1995) 397–410.
- [33] E.H. Hauri, S.R. Hart, Re–Os isotope systematics of HIMU and EMII oceanic island basalts from the south Pacific Ocean, *Earth Planet. Sci. Lett.* 114 (1993) 353–371.
- [34] C.E. Martin, R.W. Carlson, S.B. Shirey, F.A. Frey, C.-Y. Chen, Os isotopic variation in basalts from Haleakala volcano, Maui, Hawaii: a record of magmatic processes in oceanic mantle and crust, *Earth Planet. Sci. Lett.* 128 (1995) 287–301.
- [35] M. Roy-Barman, C.J. Allègre, $^{187}\text{Os}/^{186}\text{Os}$ ratios of mid-ocean ridge basalts and abyssal peridotites, *Geochim. Cosmochim. Acta* 58 (1994) 5043–5054.
- [36] J.M. Hertogen, J. Janssens, H. Palme, Trace elements in ocean ridge basalt glasses: implications for fractionations during mantle evolution and petrogenesis, *Geochim. Cosmochim. Acta* 44 (1980) 2125–2143.
- [37] J.E. Snow, L.R. Reisberg, Os isotope systematics of the MORB mantle: results from altered abyssal peridotites, *Earth Planet. Sci. Lett.* 133 (1995) 411–421.
- [38] A.D. Brandon, R.A. Creaser, S.B. Shirey, R.W. Carlson, Osmium recycling in subduction zones, *Science* 272 (1996) 861–864.
- [39] T. Meisel, R.J. Walker, J.W. Morgan, The osmium isotopic composition of the Earth's primitive upper mantle, *Nature (London)* 383 (1996) 517–520.
- [40] B.D. Marsh, Some Aleutian andesites: their nature and source, *J. Geol.* 84 (1976) 27–45.
- [41] T.L. Wright, M. Mangan, D.A. Swanson, Chemical data for flows and feeder dikes of the Yakima basalt subgroup, Columbia River basalt group, Washington, Oregon, and Idaho, and their bearing on a petrogenetic model, *U.S. Geol. Surv. Bull.* 1821 (1989) 1–71.
- [42] A.D. Smith, Back-arc convection model for Columbia River basalt genesis, *Tectonophysics* 207 (1992) 269–285.
- [43] R.W. Carlson, S. Esperança, D.P. Svisero, Chemical and Os isotopic study of Cretaceous potassic rocks from southern Brazil, *Contrib. Mineral. Petrol.* 125 (1996) 393–405.
- [44] A. Yasuda, T. Fujii, K. Kurita, Melting phase relations of an anhydrous mid-ocean ridge basalt from 3 to 20 GPa: implications for the behavior of subducted oceanic crust in the mantle, *J. Geophys. Res.* 99 (1994) 9401–9414.
- [45] A. Carlson, Isotopic constraints on Columbia River flood basalt genesis and the nature of the subcontinental mantle, *Geochim. Cosmochim. Acta* 48 (1984) 3257–3272.
- [46] S. Esperança, R.W. Carlson, S.B. Shirey, D. Smith, Dating crust–mantle separation: Re–Os isotopic study of mafic xenoliths from central Arizona, *Geology* (1997) in press.